On the Role of Moist Processes in Tropical Intraseasonal Variability: Cloud–Radiation and Moisture–Convection Feedbacks

SANDRINE BONY

Laboratoire de Météorologie Dynamique, Institut Pierre-Simon Laplace, CNRS, Paris, France

KERRY A. EMANUEL

Program for Atmospheres, Oceans and Climate, Massachusetts Institute of Technology, Cambridge, Massachusetts

(Manuscript received 3 May 2004, in final form 21 December 2004)

ABSTRACT

Recent observations of the tropical atmosphere reveal large variations of water vapor and clouds at intraseasonal time scales. This study investigates the role of these variations in the large-scale organization of the tropical atmosphere, and in intraseasonal variability in particular. For this purpose, the influence of feedbacks between moisture (water vapor, clouds), radiation, and convection that affect the growth rate and the phase speed of unstable modes of the tropical atmosphere is investigated.

Results from a simple linear model suggest that interactions between moisture and tropospheric radiative cooling, referred to as moist-radiative feedbacks, play a significant role in tropical intraseasonal variability. Their primary effect is to reduce the phase speed of large-scale tropical disturbances: by cooling the atmosphere less efficiently during the rising phase of the oscillations (when the atmosphere is moister) than during episodes of large-scale subsidence (when the atmosphere is drier), the atmospheric radiative heating reduces the effective stratification felt by propagating waves and slows down their propagation. In the presence of significant moist-radiative feedbacks, planetary disturbances are characterized by an approximately constant frequency. In addition, moist-radiative feedbacks excite small-scale disturbances advected by the mean flow. The interactions between moisture and convection exert a selective damping effect upon small-scale disturbances, thereby favoring large-scale propagating waves at the expense of small-scale advective disturbances. They also weaken the ability of radiative processes to slow down the propagation of planetary-scale disturbances. This study suggests that a deficient simulation of cloud radiative interactions or of convection-moisture interactions may explain some of the difficulties experienced by general circulation models in simulating tropical intraseasonal oscillations.

1. Introduction

Observations have revealed a dominant mode of variability of the tropical atmosphere at intraseasonal time scales. In particular, a phenomenon now referred to as the Madden–Julian oscillation (MJO; Madden and Julian 1971, 1972) is characterized by a preponderance of eastward propagating planetary-scale disturbances (wavenumbers 1–3) confined to within $\pm 30^\circ$ of latitude of the equator and having a period of 30–60 days. Besides its influence in the modulation of the tropical weather and cyclone activity (Maloney and Hartmann 2000), the MJO presumably has a role in the onset, bursts, and break periods of the Indian and Australian monsoons, and is likely to be involved in tropical interannual variability (see Madden and Julian 1994 for a review). Understanding and predicting this phenomenon therefore constitutes a major meteorological challenge that may have important implications for seasonal forecasting of tropical climate.

The physical processes responsible for the intraseasonal variability of the tropical atmosphere remain largely enigmatic, however. The different theories that have been proposed to explain the origin and the characteristics of the MJO (see Lin et al. 2000 for a review) have difficulties in explaining every aspect of the phenomenon: the instability mechanism responsible for initiating large-scale disturbances, the mechanism responsible for the maintenance of the disturbance against

Corresponding author address: Sandrine Bony, LMD/IPSL, UPMC, case courrier 99, 4 place Jussieu, 75252 Paris Cedex 05, France.
E-mail: bony@lmd.jussieu.fr

dissipation, the propagation characteristics (in particular its low phase speed), the selectivity of planetary scales, and the tropical but not exclusively equatorial manifestation of the phenomenon. These difficulties, especially the problem of low phase speed and low wavenumber structure, plus the poor representation of the MJO in atmospheric general circulation models (GCMs) demonstrated by Slingo et al. (1996), led to speculations that one or several fundamental processes essential to the MJO could be lacking or misrepresented in current theories and GCMs.

The role in 30–60-day tropical oscillations of enthalpy exchanges between the surface and the atmosphere has been extensively studied (e.g., Neelin et al. 1987; Emanuel 1987). Subsequently, the role of interactions between the ocean and the atmosphere on intraseasonal time scales has been emphasized (e.g., Flatau et al. 1997; Sperber et al. 1997; Wang and Xie 1998; Waliser et al. 1999; Woolnough et al. 2000). More recently, observational and numerical studies have focused on intraseasonal variations of tropospheric moisture (water vapor, clouds) and on their potential role in the organization of tropical convection through radiative and convective feedbacks (Raymond 2001; Tompkins 2001; Fuchs and Raymond 2002; Myers and Waliser 2003; Sperber 2003; Grabowski 2003; Grabowski and Moncrieff 2004, hereafter GM04).

Observational studies reveal that in regions of significant intraseasonal variability, such as the Indian and the western Pacific Oceans, tropospheric radiative cooling undergoes large temporal variations on intraseasonal time scales, in concert with cloud variations (Mehta and Smith 1997; Johnson and Ciesielski 2000). Indeed, by absorbing infrared radiation and subsequently reemitting it at lower temperatures, clouds and water vapor contribute to the atmospheric greenhouse effect and thereby exert a warming effect within the troposphere. The higher the altitude of water molecules, the larger the magnitude of this effect. Therefore, the reduction of the tropospheric cooling by the greenhouse effect is particularly strong in tropical regions where convection moistens the upper troposphere and gives rise to extensive upper level clouds.[1] Intraseasonal variations of cloud cover and outgoing longwave radiation have long been considered as manifestations of the intraseasonal variability of atmospheric convection. Reciprocally, the question arises as to what extent cloud–radiation interactions may rectify the intraseasonal variability of the Tropics.

Numerical studies that address this issue provide contrasting results. Using a GCM, Slingo and Madden (1991) found that the radiative warming of upper tropospheric clouds damped the intraseasonal oscillations simulated by their model, but had no significant influence on their period. By contrast, Lee et al. (2001) showed that in their GCM, cloud–radiation interactions significantly affect the simulation of tropical intraseasonal oscillations. Recent experiments conducted with the Massachusetts Institute of Technology (MIT) GCM, using a parameterization of the cloudiness coupled to the convection and carefully evaluated against Tropical Ocean Global Atmosphere Coupled Ocean–Atmosphere Response Experiment (TOGA COARE) data (Bony and Emanuel 2001), also reveal a significant influence of cloud–radiation interactions on the simulation of tropical intraseasonal oscillations (Zurovac-Jevtic et al. 2005, manuscript submitted to *J. Atmos. Sci.*). Using a numerical model of intermediate complexity, Raymond (2001) found that cloud–radiation interactions provide an instability mechanism necessary to create global-scale tropical modes reminiscent of the MJO. Numerical experiments performed with a cloud-resolving model suggest that while cloud-radiative interactions have a significant effect on the large-scale convective organization and its scale-dependence, they are apparently not necessary for getting MJO-like oscillations (Grabowski and Moncrieff 2002). The role that cloud–radiation interactions may play in tropical intraseasonal variability thus appears to be model dependent. This is consistent with the fact that the numerical representation of macrophysical and microphysical cloud processes and their interaction with radiation vary widely among GCMs, as well as among cloud-resolving models.

Besides its radiative influence, atmospheric moisture interacts with convection in several ways: while the boundary layer humidity controls the total water content and buoyancy of ascending parcels, the free tropospheric moisture affects the rate at which clouds lose buoyancy through entrainment of unsaturated air into the convective column. Moreover, the intensity of convective downdrafts driven by reevaporation of the falling precipitation, and the efficiency of these fluxes in injecting low-entropy air into the subcloud layer strongly depends on the degree of saturation of both the lower and middle troposphere. The TOGA COARE experiment revealed spectacular examples of interactions between convection and moisture, with the inhibition of cumulus convection following the arrival

[1] In the upper troposphere, the absorption of solar radiation by clouds also contributes to radiative warming of the troposphere. Nevertheless, observations show that cloud–longwave effects constitute the primary modulators of the tropospheric radiative cooling on intraseasonal time scales (Mehta and Smith 1997; Johnson and Ciesielski 2000).

of a dry intrusion and the progressive recovery to moist conditions of the middle troposphere by convective moistening (Parson et al. 2000; Redelsperger et al. 2002). Observations reveal complex patterns of water vapor variations at intraseasonal time scales (Myers and Waliser 2003; Sperber 2003). As for cloud–radiation interactions, the question arises whether these variations play an active role in the large-scale organization of tropical convection, and in the MJO in particular. Recent numerical experiments representing atmospheric convection through a parameterization or a cloud-resolving model suggest this might well be the case (Tompkins 2001; Woolnough et al. 2001; Grabowski 2003; GM04).

The aim of this study is to investigate further whether and how the interaction of moisture and cloud variations with radiation and convection may affect the intraseasonal variability of the Tropics. For this purpose, we include in a linear model of the tropical atmosphere a simple but physically based representation of radiative processes and the coupling between precipitation efficiency and the degree of saturation of the troposphere (section 2). We use this model to investigate how the feedbacks between moisture and radiation (section 3), and between moisture and convection (section 4) affect the growth rate and the phase speed of unstable modes of a simple, nonrotating atmosphere. In section 5, we summarize our results and discuss both their relevance and their limitations for understanding phenomena actually observed in the tropical atmosphere or in numerical simulations.

TABLE 1. List of symbols and variables used in the linear model of the tropical atmosphere.

u	Zonal wind at the top of the subcloud layer
U	Mean zonal wind
w_c	Vertical velocity in the deep convective area
w_d	Vertical velocity in the environment
σ	Fractional areal coverage of cumulus convection
$w = \sigma w_c + (1 - \sigma)w_d$	Total vertical velocity
Φ	Geopotential
θ	Average tropospheric potential temperature
θ_{eb}	Equivalent potential temperature of the subcloud layer
θ_{em}	Average equivalent potential temperature of the troposphere
ε_p	Precipitation efficiency
$\dot{R}$	Radiative cooling rate ($-\dot{R}$ is the radiative heating rate)
α	Intensity factor of moisture–radiation interactions
γ	Intensity factor of moisture–precipitation efficiency interactions
$a = 6.38\ 10^6$ m	Radius of the earth
$g = 9.8$	Gravitational acceleration
$N^2 = 10^{-4}$ s^{-2}	*N:* buoyancy frequency of dry air
$H_f = 8$ km	Thickness of the troposphere
$H_m = 5$ km	Level of minimum θ_e in the troposphere
$h = 500$ m	Thickness of the subcloud layer
$C_k = 1.2 \times 10^{-3}$	Bulk coefficient of entropy exchange
$C_d = 1.0 \times 10^{-3}$	Bulk coefficient of momentum exchange rate
$\bar{\varepsilon} = 0.1$	Thermodynamic efficiency
$\overline{T}$	Mass-weighted tropospheric averaged temperature
T_b	Mean temperature at the top of the subcloud layer
$\ln(\overline{\theta_{es}}/\overline{\theta_{eb}}) = 0.035$	Thermodynamic disequilibrium
$\lvert U\rvert = 5$ m s^{-1}	Magnitude of the mean zonal wind
$C_p = 1000$ J kg^{-1} K^{-1}	Specific heat at constant pressure
$\Gamma = \Gamma_{dry}/\Gamma_{moist} = 1.7$	Ratio of dry and moist adiabatic temperature lapse rates

2. Linear model of the tropical atmosphere

a. Physics of the model

We use the simple two-layer linear model of the tropical atmosphere proposed by Emanuel (1987) and improved by Yano and Emanuel (1991) and Emanuel (1993). We restrict it to the equator and to two-dimensions (the meridional component of the wind is zero), and we neglect the coupling with the stratosphere. The goal here is to explore the basic nature of physical interactions, not to simulate specific tropical phenomena.

We recall here the main basic features of this model. The meaning of the different symbols used in the model's equations is given in Table 1. Following Emanuel (1987), the tropical atmosphere is consisting of a thin subcloud layer and a deep free troposphere. The boundary layer and the free troposphere interact through vertical motions composed, on the one hand, by convective fluxes and, on the other hand, by gentle subsidence occurring in the quiescent environment surrounding convective systems. Different kinds of convective fluxes are considered: a deep precipitating updraft (M_c), a shallow updraft (M_{su}) that idealizes nonprecipitating saturated updrafts, and a shallow downdraft (M_{sd}) that represents both saturated downdrafts associated with nonprecipitating convection and unsaturated downdrafts driven by rain evaporation. We assume that the shallow updraft and downdraft are of equal mass flux ($M_s = M_{su} = -M_{sd}$). With that assumption, the net convective mass flux equals the deep convective mass flux, and the total convective updraft ($M^{\uparrow} = M_c + M_s$) is linearly related to the convective down-

draft ($M_\downarrow = -M_s$) by the relationship $M^\downarrow = -(1 - \varepsilon_p)M^\uparrow$, where ε_p is a precipitation efficiency defined as the ratio of the deep upward mass flux to the total updraft mass flux:

$$\varepsilon_p = M_c/(M_c + M_s). \tag{1}$$

If σ is the fractional area covered by deep cumulus convection, w_c the vertical velocity in deep convective regions, and w_d the vertical velocity in the environment, then the ensemble average vertical velocity is given by

$$w = \sigma w_c + (1 - \sigma)w_d, \tag{2}$$

with $\sigma w_c = M^\uparrow + M^\downarrow = M_c$.

The atmosphere is considered to have a moist adiabatic temperature lapse rate (its vertical structure is reduced to the first baroclinic mode), and θ is the potential temperature averaged over the troposphere. The conservation of dry entropy ($C_p \ln\theta$) in the free troposphere is expressed as

$$\left(\frac{\partial}{\partial t} + u_b\frac{\partial}{\partial x} + w\frac{\partial}{\partial z}\right)C_p \ln\theta = \dot{Q}_{\text{conv}} + \dot{Q}_{\text{rad}},$$

where u_b is the zonal wind at the top of the subcloud layer, $\dot{Q}_{\text{conv}}$ is the vertically averaged convective heating, and $\dot{Q}_{\text{rad}}$ the net tropospheric radiative heating. The convective heating may be approximated by the tropospheric warming associated with the subsidence induced by deep convective mass fluxes, $\dot{Q}_{\text{conv}} \approx \sigma w_c \partial(C_p \ln\theta)/\partial z$. Noting that $N^2 = g(\partial \ln\theta/\partial z)$, and defining the radiative cooling rate of the troposphere as $\dot{R} = -(\dot{Q}_{\text{rad}}/C_p)$, we get the thermodynamic equation

$$g\left(\frac{\partial}{\partial t} + u_b\frac{\partial}{\partial x}\right)\ln\theta = N^2(-w + \sigma w_c) - g\dot{R}. \tag{3}$$

The three terms on the right-hand side of (3) represent the effect on tropospheric temperature of large-scale adiabatic motions, of convective heating and radiative cooling, respectively.

Following Yano and Emanuel (1991), we now express the moist entropy budget of the free troposphere and of the subcloud layer. The free troposphere loses entropy through radiation and gains entropy from the subcloud layer through shallow convective updrafts and from the upper troposphere through downward advection in the environment. Noting that the moist entropy of the upper troposphere equals that of the subcloud layer owing to moist convective neutrality, and using (1) and (2), this can be written as

$$H_f\left(\frac{\partial}{\partial t} + u_b\frac{\partial}{\partial x}\right)\ln\theta_{\text{em}} = -H_f\dot{R} - \left(w - \frac{\sigma w_c}{\varepsilon_p}\right)(\ln\theta_{\text{eb}} - ln\theta_{\text{em}}), \tag{4}$$

where θ_{em} is the average equivalent potential temperature of the free troposphere and H_f is the depth of the free troposphere. The subcloud layer gains entropy from surface fluxes and exchanges entropy with the free troposphere and the upper troposphere through convective fluxes and downdraft advection in the environment:

$$h\left(\frac{\partial}{\partial t} + u_b\frac{\partial}{\partial x}\right)\ln\theta_{\text{eb}} = C_k|\mathbf{V}_b|(\ln\theta_{\text{es}} - \ln\theta_{\text{eb}}) + \left(w - \frac{\sigma w_c}{\varepsilon_p}\right)(\ln\theta_{\text{eb}} - \ln\theta_{\text{em}}), \tag{5}$$

where h is the thickness of the subcloud layer, θ_{eb} is the equivalent potential temperature of the subcloud layer, and $|\mathbf{V}_b|$ refers to the magnitude of the horizontal wind at the top of the subcloud layer (Table 1).

The momentum equation in the equatorial plane is expressed as

$$\left(\frac{\partial}{\partial t} + u_b\frac{\partial}{\partial x}\right)u_b = -\frac{\partial\Phi_b}{\partial x} - \frac{C_d}{h}|\mathbf{V}_b|u_b, \tag{6}$$

where Φ_b is the geopotential at the top of the subcloud layer. As explained in Emanuel (1987), Yano and Emanuel (1991), and Emanuel (1993), the condition of moist neutrality of the troposphere plus the vertical integration of the hydrostatic relation allows to relate the fluctuations of Φ_b to the fluctuations of the subcloud-layer moist entropy $\delta\Phi_b = -C_p(T_b - \overline{T})\delta\ln\theta_{\text{eb}}$ where T_b and $\overline{T}$ are temperatures at the top of the subcloud layer and averaged over the troposphere, respectively.

Finally, the mass continuity equation, evaluated at the middle level of the model, is given by

$$\frac{\partial u_b}{\partial x} + \frac{w}{H_m} = 0. \tag{7}$$

b. Linearized nondimensional equations

To investigate the linear instability of the system, we now linearize these equations around a mean basic state. We assume this mean basic state is characterized by a vertically and horizontally uniform easterly wind U and no mean vertical motion ($[w] = 0$). Using (4) and (5), we get

$$[\dot{R}] = \frac{C_k|U|\ln[\theta_{\text{es}}/\theta_{\text{eb}}]}{H_f}, \tag{8}$$

where brackets denote basic-state values. This expresses the balance between entropy loss by radiation and entropy gain from surface fluxes of the tropo-

sphere. The thermodynamic equation leads to $[\sigma w_c]N^2/g = [\dot{R}]$, which simply expresses the equilibrium between radiative and convective heating of the troposphere. Using (5), we have then

$$[\ln\theta_{eb} - \ln\theta_{em}] = \varepsilon_p N^2 H_f/g. \tag{9}$$

We look for solutions of the form $e^{ikx+\omega t}$. Using the scaling and nondimensional parameters of Yano and Emanuel (1991) recalled in Tables 2 and 3, and noting that the linear perturbation of $|\mathbf{V}_b|$ is given by $u\,\mathrm{sgn}(U)$, the linearized form of the equations for zonal wind, vertical velocity, deep convective mass flux, and entropy perturbations on the basic state are given by

$$(D + 2F)u = ikT_{eb}, \tag{10}$$

$$iku + w = 0, \tag{11}$$

$$D\frac{T_{eb}}{\Gamma} = \lambda(-w + \sigma w_c) - \delta\tilde{\dot{R}}, \tag{12}$$

$$DT_{em} = \lambda(-\varepsilon_p w + \sigma w_c) + \alpha_D(T_{eb} - T_{em}) - \delta\tilde{\dot{R}}, \tag{13}$$

$$\frac{h}{H_f}DT_{eb} = \mathrm{sgn}(U)u - \alpha_E T_{eb} + \lambda(\varepsilon_p w - \sigma w_c) - \alpha_D(T_{eb} - T_{em}), \tag{14}$$

where every quantity in these equations is a perturbation, where $D \equiv ikU + \omega$ has been introduced, and where $\delta\tilde{\dot{R}} = (a^{1/2}A^{-1/2}/\Delta)\delta\dot{R}$ is the nondimensional linearized perturbation of the radiative cooling whose expression will be developed in the next section.

The condition of quasi equilibrium for the subcloud-layer entropy, which expresses the quasi balance between the tendency of surface fluxes and convective downdrafts to increase and decrease the subcloud-layer entropy (Raymond 1995), amounts to neglecting the left-hand side of (14) (or $h/H_f \ll 1$). Using the linearized version of this equation, this condition yields the following diagnostic relation for the cumulus mass flux:

TABLE 2. Nondimensionalization of the different variables of the linear model (variables with asterisks are dimensional, those without asterisks are nondimensional).

x^*	$= ax$
t^*	$= a^{1/2}A^{-1/2}t$
u^*	$= a^{1/2}A^{1/2}u$
w^*	$= H_m a^{-1/2}A^{1/2}w$
$\delta\Phi^*$	$= -aAT_{eb}$
$\delta\ln\theta^*$	$= \Delta T_{eb}/\Gamma$
$\delta\ln\theta^*_{eb}$	$= \Delta T_{eb}$
$\delta\ln\theta^*_{em}$	$= \Delta T_{em}$

TABLE 3. Nondimensional parameters used in the linearized equations for perturbations (after Yano and Emanuel 1991).

A	$= \bar{\varepsilon}C_p T_b C_k H_f^{-1}\ln(\overline{\theta_{es}}/\overline{\theta_{eb}})$
Δ	$= aH_f^{-1}C_k\ln(\overline{\theta_{es}}/\overline{\theta_{eb}})$
λ	$\equiv (N^2H_m)/(g\Delta)$
α_E	$\equiv C_k\lvert U^*\rvert a^{1/2}A^{-1/2}/H_f$
α_D	$\equiv \dfrac{a^{1/2}A^{-1/2}C_k\lvert U^*\rvert}{\varepsilon_p H_f^2 N^2} g\ln\left(\dfrac{\overline{\theta_{es}}}{\overline{\theta_{eb}}}\right)$
F	$\equiv C_d\lvert U^*\rvert a^{1/2}A^{-1/2}/h$

$$\sigma w_c = \varepsilon_p w + \frac{1}{\lambda}\{\mathrm{sgn}(U)u - \alpha_E T_{eb}\} - \frac{1}{\lambda}\alpha_D(T_{eb} - T_{em}). \tag{15}$$

This equation expresses the response of convection to a change in the large-scale ascent (first rhs term), in surface fluxes (second rhs term) or in the entropy difference between the subcloud layer and the free troposphere (last term).

Emanuel (1993), Neelin and Yu (1994), and Yu and Neelin (1994) showed that accounting for the finite response time of convection (which corresponds to the time scale for the growth of convective clouds and the time that precipitation processes take to become fully efficient) can have a strong effect on the scale selectivity of waves. Following Emanuel (1993), we introduce a Galilean invariant convective delay τ_c of a few hours by evaluating the convective mass flux σw_c at a time $t - \tau_c$:

$$\sigma w_c = \left(\varepsilon_p w + \frac{1}{\lambda}\{\mathrm{sgn}(U)u - \alpha_E T_{eb}\} - \frac{1}{\lambda}\alpha_D(T_{eb} - T_{em})\right)_{t-\tau_c}, \tag{16}$$

which can also be written as

$$\sigma w_c = \left(\varepsilon_p w + \frac{1}{\lambda}\{\mathrm{sgn}(U)u - \alpha_E T_{eb}\} - \frac{1}{\lambda}\alpha_D(T_{eb} - T_{em})\right)e^{-D\tau_c}. \tag{17}$$

With τ_c being short compared to the time scale of disturbances we are interested in ($|D\tau_c| \ll 1$), in the following $e^{-D\tau c}$ will be approximated at first order by $1 - D\tau_c$.

c. Representation of radiative processes

Yano and Emanuel (1991) represented the radiative cooling term $\dot{R}$ as a Newtonian cooling that damped temperature perturbations over a time scale of about 50 days. However, observations reveal that in the Western Hemisphere, the passage of intraseasonal oscillations

(ISO) is associated with tropospheric radiative cooling variations of ±150% (Johnson and Ciesielski 2000), top-of-atmosphere (TOA) outgoing longwave radiation (OLR) variations of several tens of W m^{-2} (Yanai et al. 2000), but tropospheric temperature variations of only a few tenths of a degree (Johnson and Ciesielski 2000). Typical sensitivities of the OLR to temperature variations can be estimated from basic considerations of radiative transfer. The Planck relationship states that the emitted longwave flux depends on temperature as σT^4, where σ is the Stefan–Boltzmann constant. Its sensitivity to temperature is thus given by $4\sigma T^3$. As atmospheric temperatures are less than about 300 K, sensitivities to temperature are less than about 6 W m^{-2} K^{-1}. Observed temperature variations can thus account for only a small part of intraseasonal radiative perturbations. In other words, OLR or radiative cooling variations are not primarily due to variations in atmospheric temperature, but to variations in infrared atmospheric opacity. Clouds and humidity therefore constitute the main modulators of the radiation field in tropical convective atmospheres.

We thus neglect the interaction of $\dot{R}$ with temperature and focus on its interaction with moisture. (By moisture, we mean atmospheric water in all its phases, including water vapor and clouds). Qualitatively, we want the radiative cooling to reproduce the fact that moistening (i.e., a moister or more cloudy atmosphere) leads to larger opacity of the atmosphere, an elevation of the mean radiating height (which would be zero if the atmosphere were totally dry) and a decrease of the tropospheric radiative cooling, as suggested by observations (Mehta and Smith 1997; Johnson and Ciesielski 2000).

The entropy content of the free troposphere ($\ln\theta_{em}$) depends on both temperature and moisture. However, the difference of entropy between the subcloud layer and the free troposphere, $\ln\theta_{eb} - \ln\theta_{em}$, best characterizes the saturation deficit of the atmosphere: the difference increases (decreases) as the air gets drier (moister, respectively), and the difference vanishes in the case of a saturated atmosphere (which would occur in the absence of precipitation, i.e., for $\varepsilon_p = 0$). We thus parameterize the absolute value of the radiative cooling (the net radiative heating rate is $-\dot{R}$) as

$$\dot{R} = \dot{R}_0 \left\{ 1 + \alpha \frac{\delta(\ln\theta_{eb} - \ln\theta_{em})}{[\ln\theta_{eb} - \ln\theta_{em}]} \right\}, \tag{18}$$

where δ's denote perturbations from basic-state values, $\dot{R}_0$ is the basic-state value of the radiative cooling ($\dot{R}_0 = [\dot{R}] = C_k[U][\ln\theta_{es} - \ln\theta_{eb}]/H_f$), and α is a positive parameter whose value is specified.

Data collected during TOGA COARE indeed suggest a close relationship between the fluctuations of the moist entropy deficit of the troposphere, estimated as the difference between the equivalent potential temperature at 975 hPa and that averaged over the layer between 975 and 300 hPa, and the fluctuations of clouds and outgoing longwave radiation (Fig. 1). However, there is some scatter in the relationship, and the amplitude of the perturbations is far from small relative to the mean. Therefore, we recognize that representing radiative feedbacks in a linear framework by a relationship such as (18) constitutes a strong simplification. However, setting α to different values makes it possible to vary the strength of moist radiative feedbacks, and then to investigate easily the role that interactions between moisture, radiation, convection, and dynamics may play in the tropical atmosphere. Note that using the basic-state relationships of section 2b, (18) can be rewritten as $\dot{R} = \dot{R}_0 + \alpha\{\delta(\ln\theta_{eb} - \ln\theta_{em})/\tau_{moist}\}$, with $\tau_{moist} = (\varepsilon_p N^2 H_f / g\dot{R}_0)$. Using the numerical values reported in Table 1, $\tau_{moist} \approx 30$ days. Using the scaling and nondimensional parameters of Tables 2 and 3, the linearized perturbation of the radiative cooling $\delta\tilde{R}$ entering Eqs. (12)–(13) can be expressed as $\delta\tilde{R} = \alpha\alpha_D(T_{eb} - T_{em})$.

d. Precipitation efficiency

So far, we have assumed that the precipitation efficiency ε_p is constant. In nature, however, it is likely to vary with the degree of saturation of the troposphere because as the atmosphere gets closer to saturation, the reevaporation of cloud and precipitation decreases. These two features can be represented by an increase of ε_p as $\ln\theta_{eb} - \ln\theta_{em}$ decreases. We investigate the potential role of these interactions in the large-scale organization of tropical convection by introducing into our simple linear model a modulation of the precipitation efficiency by the degree of saturation of the troposphere. This is done by using, in Eqs. (4) and (5), a precipitation efficiency $\tilde{\varepsilon}_p$ defined by

$$\tilde{\varepsilon}_p = \frac{\varepsilon_p}{1 + \gamma \dfrac{\delta(\ln\theta_{eb} - \ln\theta_{em})}{[\ln\theta_{eb} - \ln\theta_{em}]}}, \tag{19}$$

where γ is a positive constant characterizing the strength of the coupling, and ε_p now refers to the basic-state value of $\tilde{\varepsilon}_p$. The term α_D $(T_{eb} - T_{em})$ then becomes $(1 + \gamma)\alpha_D$ $(T_{eb} - T_{em})$ on the right-hand side of nondimensional, linearized Eqs. (13), (14), and (15). As will be discussed more extensively in section 4, taking into account the coupling between the precipitation efficiency and the degree of saturation of the troposphere

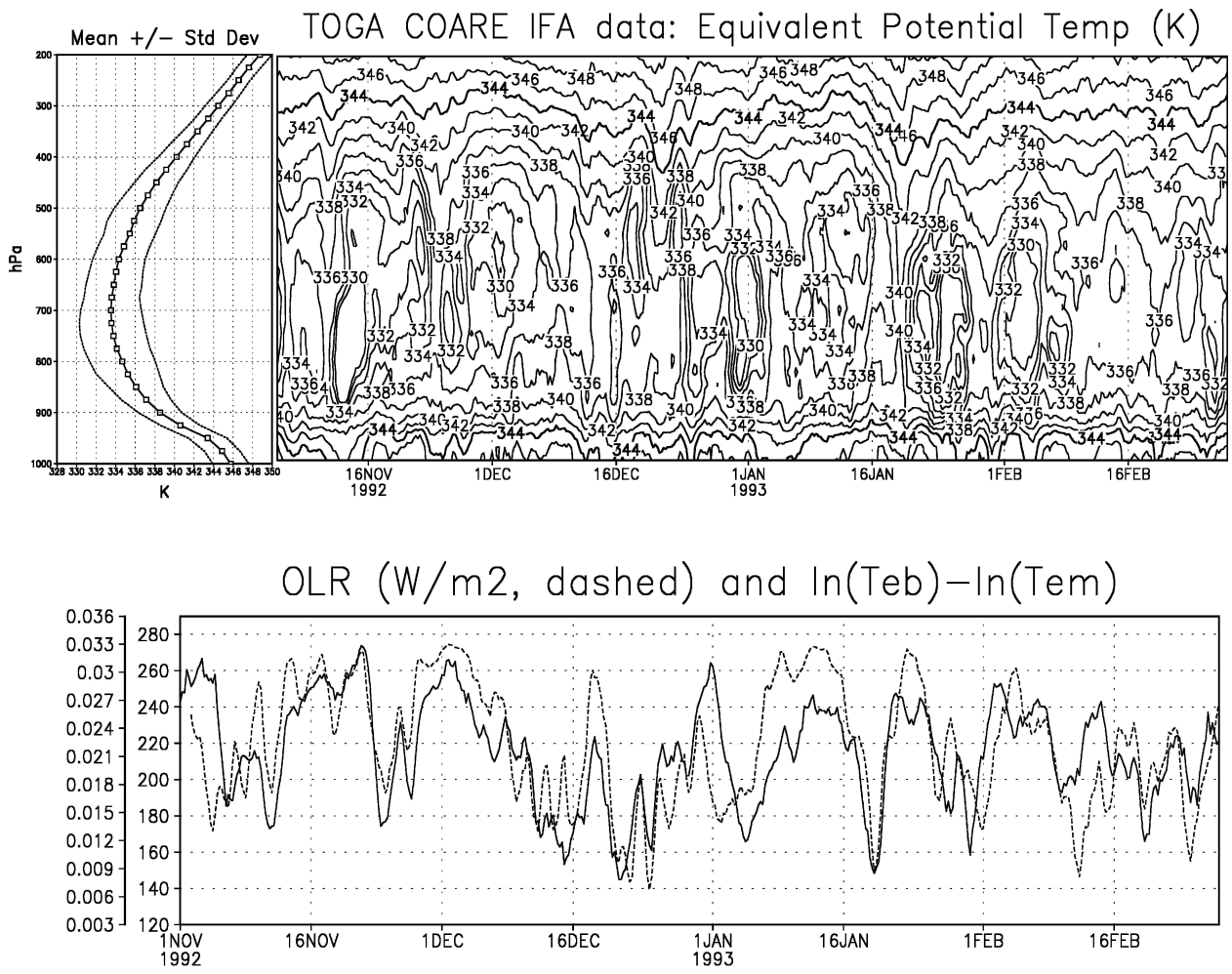

FIG. 1. (top) Time evolution of the vertical profile of moist reversible equivalent potential temperature θ_e derived from the radiosonde data collected over the western Pacific warm pool during the 120 days of the TOGA COARE experiment (Ciesielski et al. 2003). The average θ_e computed over the 120 days is shown on the left. (bottom) Time evolution of the OLR (inside y-axis scale) and moist entropy deficit (outside scale), computed as the difference of the log of θ_e at 975 hPa [$\ln(T_{\rm eb})$, assumed to be representative of the subcloud layer] and the log of θ_e averaged over the layer between 975 and 300 hPa [$\ln(T_{\rm em})$, assumed to be representative of the free troposphere].

enhances the effect of convective motions on the perturbation entropy gradient between the subcloud layer and the free troposphere and, reciprocally, makes convection more sensitive to perturbations of tropospheric moisture.

e. Dispersion equation

Taking into account the moisture-radiation and moisture-ε_p couplings, and considering that convection responds to large-scale processes with a finite delay τ_c, leads to the following system of equations:

$$(D + 2F)u = ikT_{\rm eb}, \tag{20}$$

$$iku + w = 0, \tag{21}$$

$$D\frac{T_{\rm eb}}{\Gamma} = \lambda(-w + \sigma w_c) - \alpha\alpha_D(T_{\rm eb} - T_{\rm em}), \tag{22}$$

$$DT_{\rm em} = \lambda(-\varepsilon_p w + \sigma w_c) + (1 + \gamma)\alpha_D(T_{\rm eb} - T_{\rm em}) - \alpha\alpha_D(T_{\rm eb} - T_{\rm em}), \tag{23}$$

$$\sigma w_c = \{\varepsilon_p w + \lambda^{-1}(\mathrm{sgn}(U)u - \alpha_E T_{\rm eb}) - \lambda^{-1}(1 + \lambda)\alpha_D(T_{\rm eb} - T_{\rm em})\}(1 - D\tau_c). \tag{24}$$

From (20) we have $u = [ik/(D + 2F)]T_{\rm eb}$. From (21) we have $w = [k^2/(D + 2F)]T_{\rm eb}$. From (22)–(23) we have $T_{\rm em} = T_{\rm eb}/[D + (1 + \gamma)\alpha_D][(D/\Gamma) + (1 + \gamma)\alpha_D + \lambda k^2(1 - \varepsilon_p)/(D + 2F)]$.

Finally, by expressing $\lambda\sigma w_c$ from (23) on the one hand, from (24) on the other hand, and then by setting the two expressions equal, we get after some manipulation the cubic algebraic equation

$$C_1 D^3 + C_2 D^2 + C_3 D + C_4 = 0, \tag{25}$$

with $C_i = C_i^0 + C_i^{\tau_c} + C_i^{\text{rad}} + C_i^{\gamma}$ and the following:

$$C_1^0 = \frac{1}{\Gamma}, \tag{26}$$

$$C_2^0 = \alpha_E + \alpha_D + \frac{2F}{\Gamma}, \tag{27}$$

$$C_3^0 = -ik\,\text{sgn}(U) + \alpha_E\alpha_D + \lambda k^2(1-\varepsilon_p) + 2F(\alpha_E + \alpha_D), \tag{28}$$

$$C_4^0 = -ik\,\text{sgn}(U)\alpha_D + 2F\alpha_E\alpha_D, \tag{29}$$

$$C_1^{\tau_c} = -\tau_c\left[\alpha_E + \alpha_D\left(1 - \frac{1}{\Gamma}\right)\right], \tag{30}$$

$$C_2^{\tau_c} = \tau_c\left\{-\alpha_E\alpha_D + ik\,\text{sgn}(U) + \varepsilon_p\lambda k^2 - 2F\left[\alpha_E + \alpha_D\left(1 - \frac{1}{\Gamma}\right)\right]\right\}, \tag{31}$$

$$C_3^{\tau_c} = \tau_c\alpha_D[\lambda k^2 - 2F\alpha_E + ik\,\text{sgn}(U)], \tag{32}$$

$$C_4^{\tau_c} = 0, \tag{33}$$

$$C_1^{\text{rad}} = 0, \tag{34}$$

$$C_2^{\text{rad}} = \alpha\alpha_D\left(1 - \frac{1}{\Gamma}\right), \tag{35}$$

$$C_3^{\text{rad}} = \alpha\alpha_D 2F\left(1 - \frac{1}{\Gamma}\right), \tag{36}$$

$$C_4^{\text{rad}} = -\alpha\alpha_D\lambda k^2(1-\varepsilon_p), \tag{37}$$

$$C_1^{\gamma} = -\tau_c\gamma\alpha_D\left(1 - \frac{1}{\Gamma}\right), \tag{38}$$

$$C_2^{\gamma} = \gamma\alpha_D - \tau_c\gamma\alpha_D\left[\alpha_E + 2F\left(1 - \frac{1}{\Gamma}\right)\right], \tag{39}$$

$$C_3^{\gamma} = \gamma\alpha_D(\alpha_E + 2F) + \tau_c\gamma\alpha_D[\lambda k^2 - 2F\alpha_E + ik\,\text{sgn}(U)], \tag{40}$$

$$C_4^{\gamma} = \gamma\alpha_D[-ik\,\text{sgn}(U) + 2F\alpha_E]. \tag{41}$$

The nondimensional growth rate and phase speed of the solutions of (25) are then given by $\text{Re}(D)$ and $-\text{Im}(D)/k$, respectively.

To point out the specific effect of each feedback on intraseasonal variability, in the following we activate the moisture-radiation and moisture-convection feedbacks one by one and consider a large range of feedback intensities, specified by the values of α and γ, respectively.[2]

3. Effect of the moist-radiative feedback

In the absence of radiative feedbacks ($\alpha = 0$) and assuming an instantaneous response of the convection to large-scale processes ($\tau_c = 0$), the growth rate of solution to (25) is maximum for high wavenumbers, and the phase speed of propagating modes relative to the background easterly flow exceeds 25 m s^{-1} (Fig. 2). When a finite convective response time is considered ($\tau_c = 0.1$), short waves are damped and low zonal wavenumbers (k = 1–4) are favored. These results are similar to those obtained by Yano and Emanuel (1991) and Emanuel (1993). In the absence of radiative feedbacks, the occurrence of unstable waves is owing to the interaction between surface heat fluxes and surface wind anomalies, referred to as wind-induced surface heat exchange (WISHE; Emanuel 1987) or evaporation wind feedback (Neelin et al. 1987). Indeed, the unstable modes of the system disappear when the WISHE mechanism is turned off in the model [which can be done by setting the sgn(U) terms to zero in the coefficients of the dispersion equation].

We next investigate the effect of radiation–moisture interactions ($\alpha > 0$) in isolation from the convection–moisture feedback ($\gamma = 0$). Figure 2 shows that the growth rates and phase speeds are significantly affected by these interactions, with a discontinuity occurring for α values of about 10 (and for α values slightly smaller as k increases). For α increasing from zero up to this discontinuity, the growth rate and the phase speed of planetary-scale disturbances decrease. For larger values of α, the phase speed continues to decrease while the growth rate increases with α. These effects occur more abruptly for small-scale waves. When a soft quasi-equilibrium is considered ($\tau_c = 0.1$), the behavior of large-scale waves is unchanged but small-scale waves become nonpropagating.

a. Planetary-scale disturbances

The phase speed of planetary waves decreases as the radiation-moisture interactions intensify. To explain this behavior, we show in Fig. 3 composites of wavenumber-1 modes for two values of α. In the presence of

[2] Note that $\tau_{\text{moist}}/\alpha$ and $\tau_{\text{moist}}/\gamma$ may be related to the relaxation time scale of the tropospheric saturation deficit or moisture perturbations, with $\tau_{\text{moist}} \approx 30$ days (see section 2c). Therefore, the larger the value of α or γ, the shortest the relaxation time scale. In the following, we consider values of α and γ ranging from 0 to 30, which correspond to a relaxation time scale longer than about 1 day.

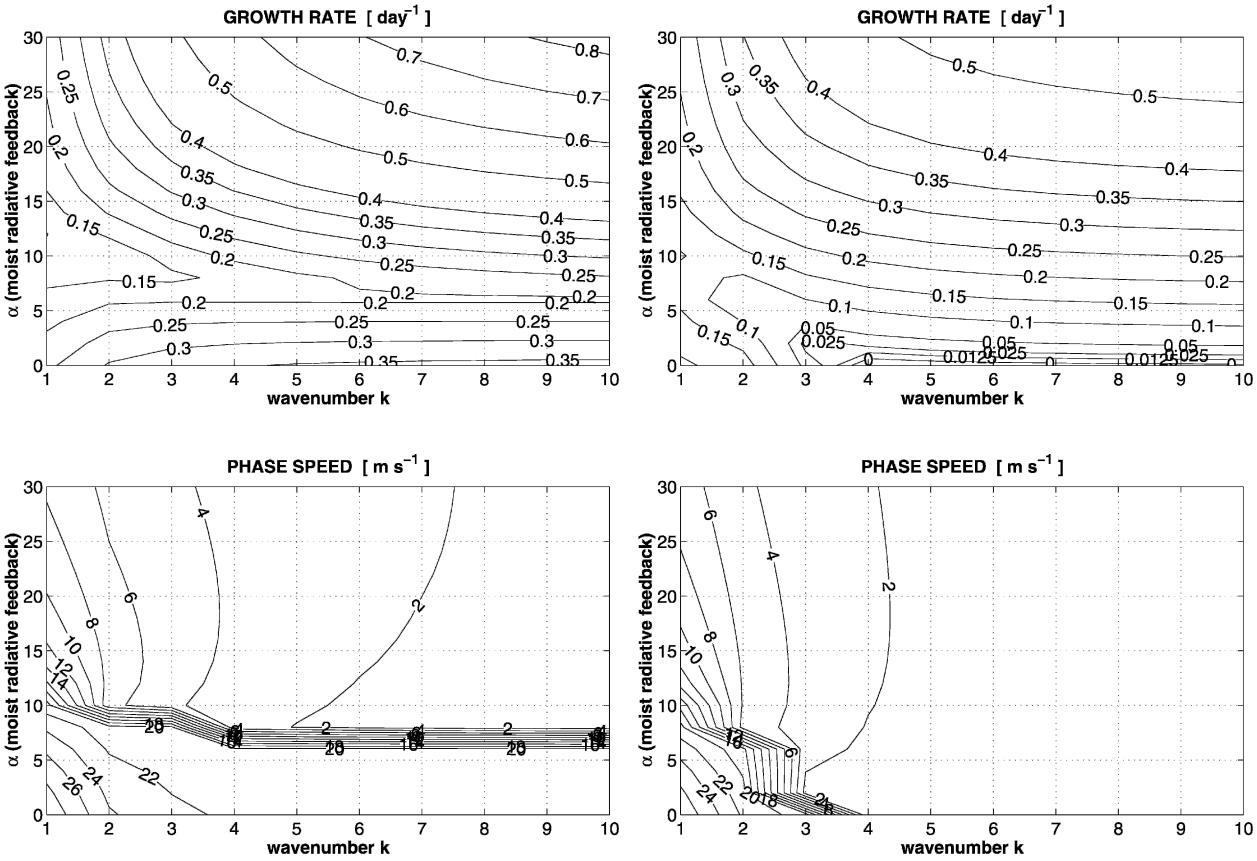

FIG. 2. (top) Growth rates and (bottom) phase speeds relative to the mean flow of the dispersion equation solutions as a function of the zonal wavenumber k and of the intensity of the moisture-radiation feedback (α) when the feedback between moisture and precipitation efficiency is turned off ($\gamma = 0$). Results are shown in the case of a strict quasi equilibrium of the convection with the large-scale flow: (left) $\tau_c = 0$, and (right) in the case of a soft quasi equilibrium, i.e., when a finite convective response time of the convection is considered: $\tau_c = 0.1$ (which corresponds to about 6 h), $F = 0$, $\varepsilon_p = 0.8$, $\overline{U} = -5$ m s^{-1}

radiation–moisture interactions, positive anomalies of radiative heating perturbations occur west of (i.e., after) the maximum large-scale ascent, in coincidence with low-level westerlies and upper-level easterlies. This heating is nearly in quadrature with vertical velocity perturbations for small values of α, but becomes more and more in phase with the large-scale ascent as α increases. This can be understood from the relative phase between the free tropospheric entropy and the wave. The basic equations of section 2a show that in the stationary state ($d\ln\theta_{\rm em}/dt = 0$), the entropy content of the middle troposphere can be expressed as

$$\ln\theta_{\rm em} = \ln\theta_{\rm eb} - \frac{(1-\alpha)\varepsilon_p C_k[U]\ln[\theta_{\rm es}/\theta_{\rm eb}]}{w(1-\varepsilon_p) - (1-\sigma)w_d - \dfrac{\alpha C_k[U] g \ln[\theta_{\rm es}/\theta_{\rm eb}]}{N^2 H_f}}. \quad (42)$$

In the absence of radiative feedbacks, large-scale ascent ($w > 0$) increases $\theta_{\rm em}$ and the degree of saturation of the troposphere. The presence of moist-radiative feedbacks ($\alpha > 1$) reinforces this increase, because of the reduction of the radiative cooling by the free tropospheric moistening. Owing to this positive feedback between large-scale ascent, atmospheric moisture, and radiation, $\theta_{\rm em}$ becomes more and more in phase with w as α increases (Fig. 4). This reduces the phase lag between moist anomalies of the middle troposphere and the wave, and thus between radiative heating anomalies and the wave. By cooling the troposphere less efficiently during events of large-scale ascent than during events of large-scale subsidence, moist-radiative processes partly oppose the thermodynamical effect of adiabatic motions. This reduces the effective stratification and slows down the propagation of planetary waves, just as the resistance of a string dictates the speed of its oscillations.

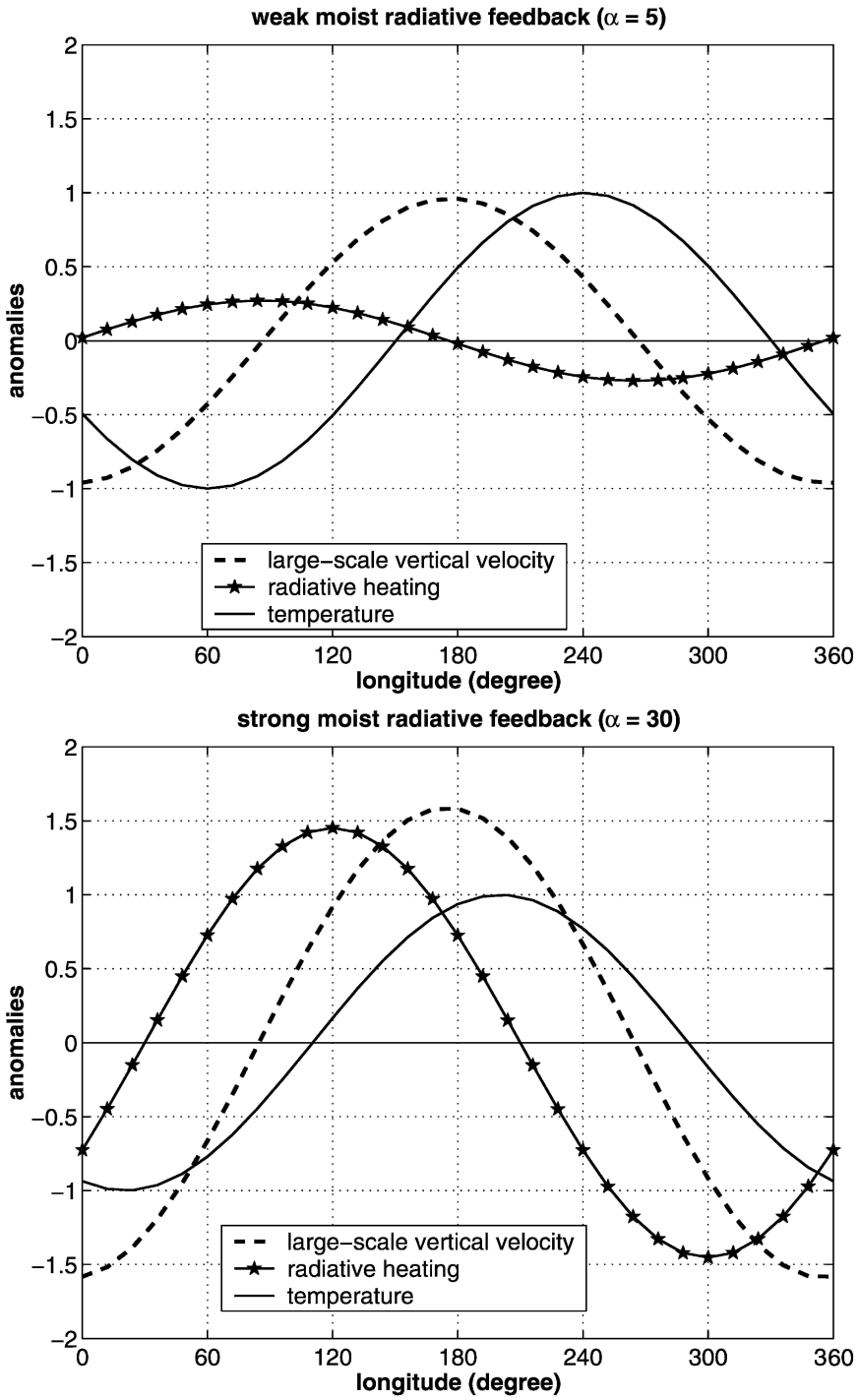

FIG. 3. Longitudinal composites of wavenumber 1 anomalies of large-scale vertical velocity (δw), radiative heating rate ($-\delta\dot{R}$), and temperature (actually, $\delta \ln \theta_{eb}$) for two values of the radiation–moisture interactions: (top) $\alpha = 5$, and (bottom) $\alpha = 30$, $\varepsilon_p = 0.8$, $\gamma = 0$, $F = 0$, $\tau_c = 0$.

In addition, by increasing the covariances $\overline{\mathrm{rad}'T'}$ and $\overline{w'T'}$, strong interactions between moisture and radiation favor the generation of potential energy and its conversion into kinetic energy, respectively. Therefore, moist-radiative feedbacks destabilize planetary-scale waves, as seen by the increase of the growth rate of low-wavenumber modes for $\alpha \gg 1$ (Fig. 2).

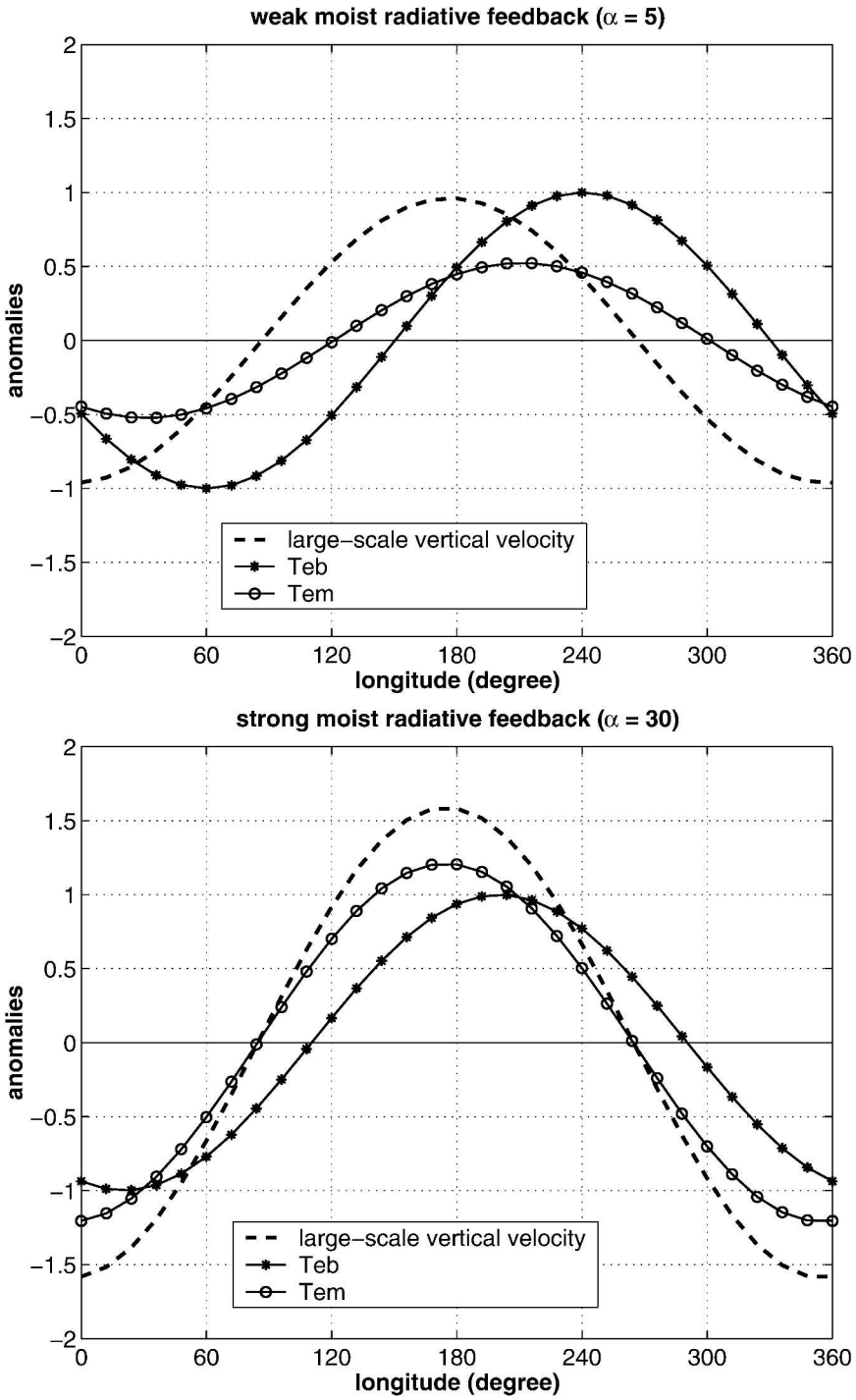

FIG. 4. As in Fig. 3 but for T_{eb} and T_{em} rather than radiative heating rate and temperature.

b. Small-scale disturbances

Figure 2 shows that high-wavenumber modes are highly sensitive to the intensity of radiation–moisture interactions. Figure 5 shows wavenumber-3 composites for two values of α that correspond to very different phase speeds of propagation: 21 m s^{-1} for $\alpha = 7$, and 5 m s^{-1} for $\alpha = 12$. In the fast wave regime, the radiative heating is almost out of phase with temperature perturbations (this decreases the growth rate) and nearly in quadrature (the covariance $\overline{\text{rad}'w'}$ is slightly positive, however) with the large-scale ascent. Radiation–

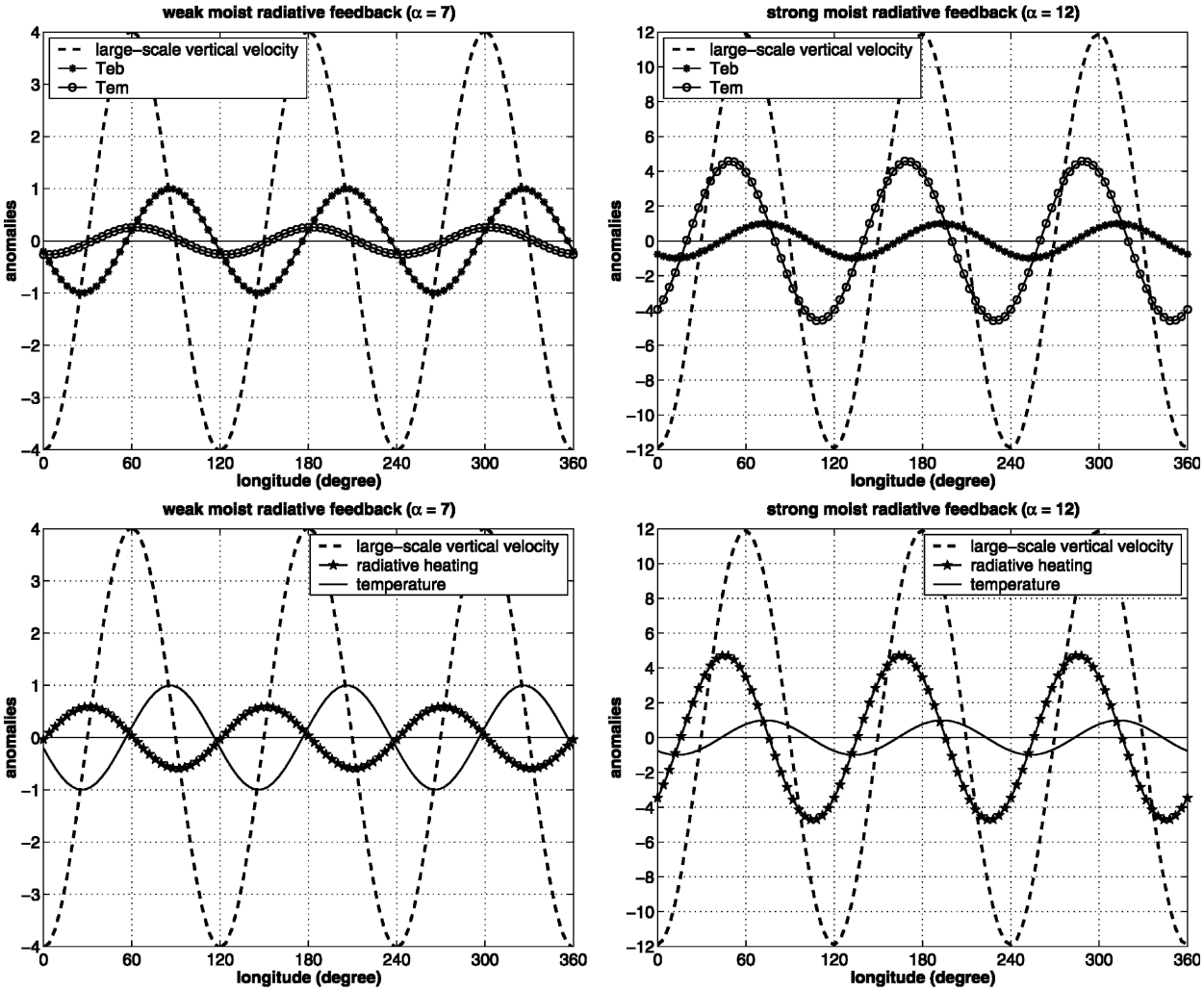

FIG. 5. As in Figs. 3 and 4 but for wavenumber 3: (left) $\alpha = 7$ and (right) $\alpha = 12$; (top) T_{eb} and T_{em} and (bottom) radiative heating rate and temperature; $\varepsilon_p = 0.8$, $\gamma = 0$, F = 0, $\tau_c = 0$.

moisture interactions thus interact very little with the large-scale motion. For stronger radiation–moisture interactions, on the other hand, the moist entropy of the free troposphere increases much more in the ascent phase of the wave, and the moistening of the atmosphere becomes more in phase with vertical velocity. The radiative warming thus occurs partly in phase with the large-scale ascent, which decreases the effective stratification and thus the phase speed. In parallel, the temperature perturbation becomes more in phase with vertical velocity, which makes these waves more unstable.

c. Surface friction

We now investigate the effect of adding some surface friction ($F \neq 0$). Qualitatively, the presence of surface friction does not affect the general nature of radiation–moisture interactions (Fig. 6). However, the transition between the fast and slow wave regimes becomes more abrupt, it occurs for weaker intensities of the radiation–moisture interactions, and the phase speed of the slow mode decreases as the surface friction increases. For wavenumber-1 disturbances, this is better shown by displaying the variation of the phase speed as a function of α for different values of the drag (Fig. 7). The transition between fast and slow modes corresponds to the case when the free tropospheric entropy becomes more variable than the subcloud-layer entropy $\{\sigma(\ln\theta_{em})/\sigma(\ln\theta_{eb}) > 1\}$.

When both a convective response time τ_c and some surface friction are considered, Figs. 6 and 7 suggest the two following main regimes:

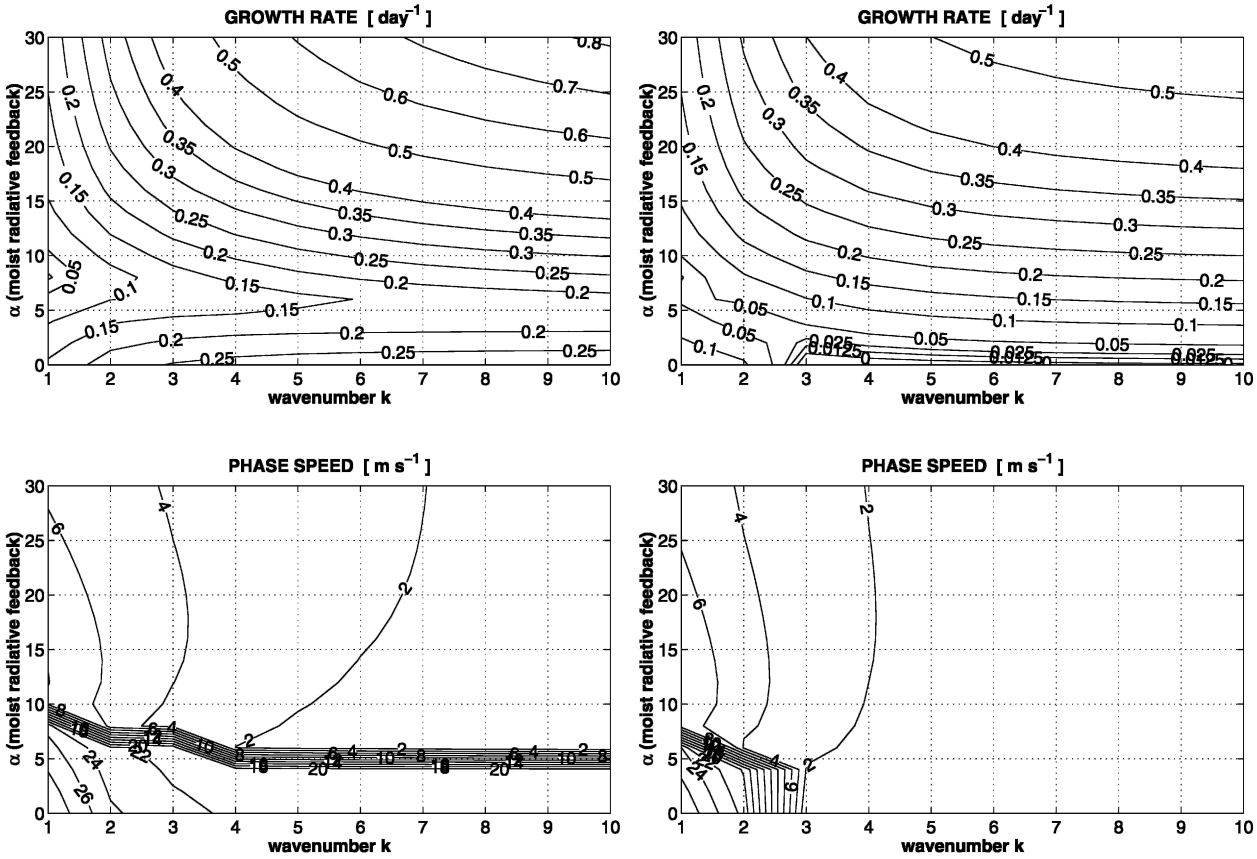

FIG. 6. As in Fig. 2 but in the presence of surface friction (F = 0.2).

- In the presence of weak radiation–moisture interactions (weak values of α), wavenumbers-1–2 disturbances are the only (or most) unstable modes; they propagate upwind at phase speeds typically larger than 20 m s^{-1} (i.e., this corresponds to a period shorter than about 23 days). In this regime, radiation–moisture interactions only slightly reduce the phase speed and slightly increase the selection of planetary-scale disturbances.
- In the presence of strong radiation–moisture interactions, two types of disturbances are destabilized: 1) small-scale advective disturbances propagating along with the mean flow (their phase speed is close to zero) and 2) slow planetary-scale disturbances propagating upwind at phase speeds ranging from a few m s^{-1} up to about 15 m s^{-1} (this corresponds to a period longer than about 30 days), depending on the intensity of radiation–moisture interactions and surface friction. The growth rate of both the small-scale and of the planetary-scale structures increases with the intensity of radiation–moisture interactions, but that of small-scale structures increases faster. The prominence of large-scale propagating disturbances over small-scale advective disturbances in the variability of the tropical atmosphere is thus likely to depend critically on the intensity of radiation–moisture interactions.

4. Effect of the moisture-convection feedback

We next investigate the influence of feedbacks between moisture and convection on the large-scale organization of the troposphere. In the absence of moist feedbacks and in conditions of strict quasi equilibrium (τ_c = 0), small-scale disturbances constitute the most unstable modes of the troposphere (see Fig. 2 for α = 0 or Fig. 8 for γ = 0). Figure 8 shows that the primary effect of the moisture-convection feedback is to damp small-scale structures and make planetary modes (k = 1–2) more prominent in the variability. We note also that the moisture-convection feedback reduces slightly the phase speed of planetary-scale disturbances. These effects remain when a soft quasi equilibrium is considered.

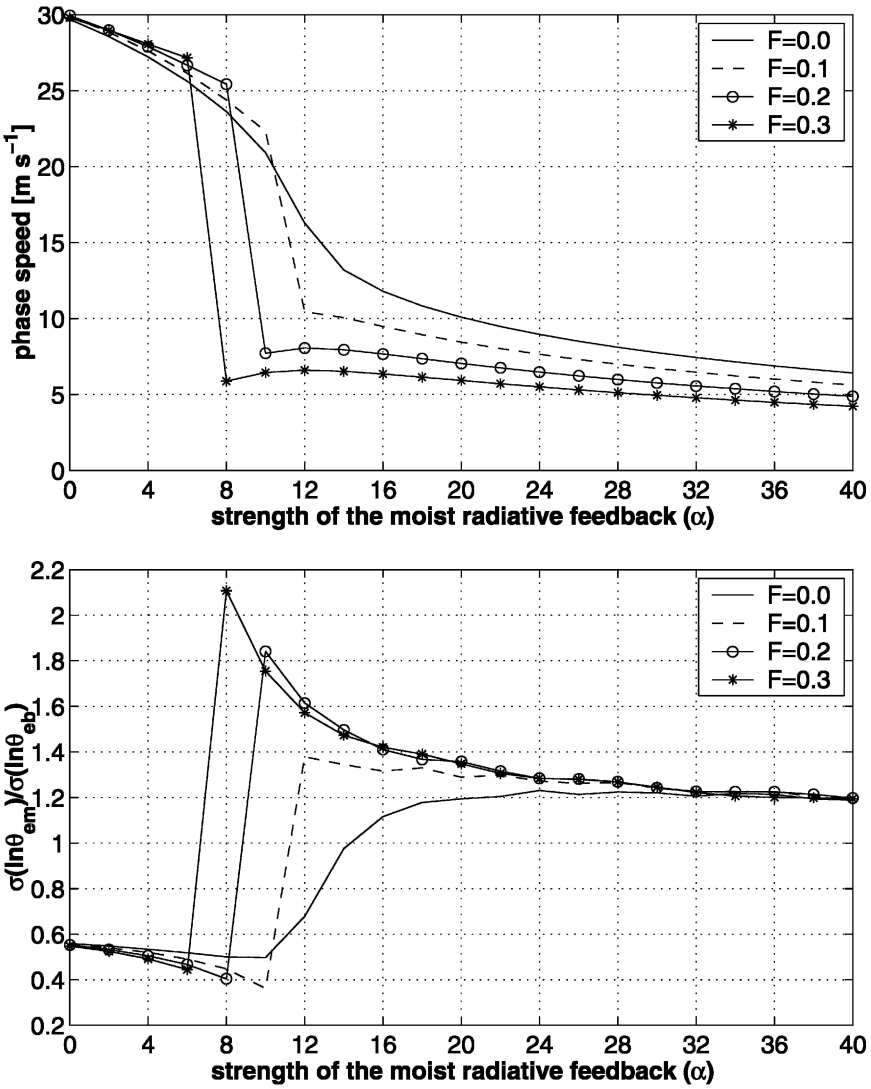

FIG. 7. Relationship between the moisture–radiation feedback strength parameter (α), and (top) the phase speed of wavenumber 1 predicted by the linear model, and (bottom) the ratio between the variances of the free tropospheric and subcloud layer moist entropies $\sigma(\ln\theta_{em})/\sigma(\ln\theta_{eb})$. Results are shown for different drag coefficients F; $\tau_c = 0.0$, $\overline{U} = -5$ m s^{-1}, $\varepsilon_p = 0.8$, $\gamma = 0$.

As moisture perturbations are likely to affect the large-scale organization of the atmosphere through both radiative and convective feedbacks, we now investigate how their presence affects the moisture-convection feedback, and vice versa. The two feedbacks decrease the phase speed of planetary-scale disturbances propagating upwind (the influence of the radiative feedback being much more dramatic than that of the moisture-convection feedback, however), but have competing influences on small-scale disturbances (Figs. 2 and 8): these latter are destabilized by radiative feedbacks, and damped by the moisture-convection feedback. Therefore, the relative prominence of small-scale structures and planetary-scale disturbances in the atmospheric spectrum is likely to depend on the relative strength of the two feedbacks. For a large range of radiative feedback intensities, the moisture-convection feedback is sufficient to make planetary-scale structures (k = 1–2) more unstable than small-scale structures (Fig. 9). Through their interaction with convection, tropospheric moisture anomalies are thus likely to play an active role in the prominence of planetary-scale disturbances in the Tropics. In the presence of strong radiative feedbacks, however, the destabilizing influ-

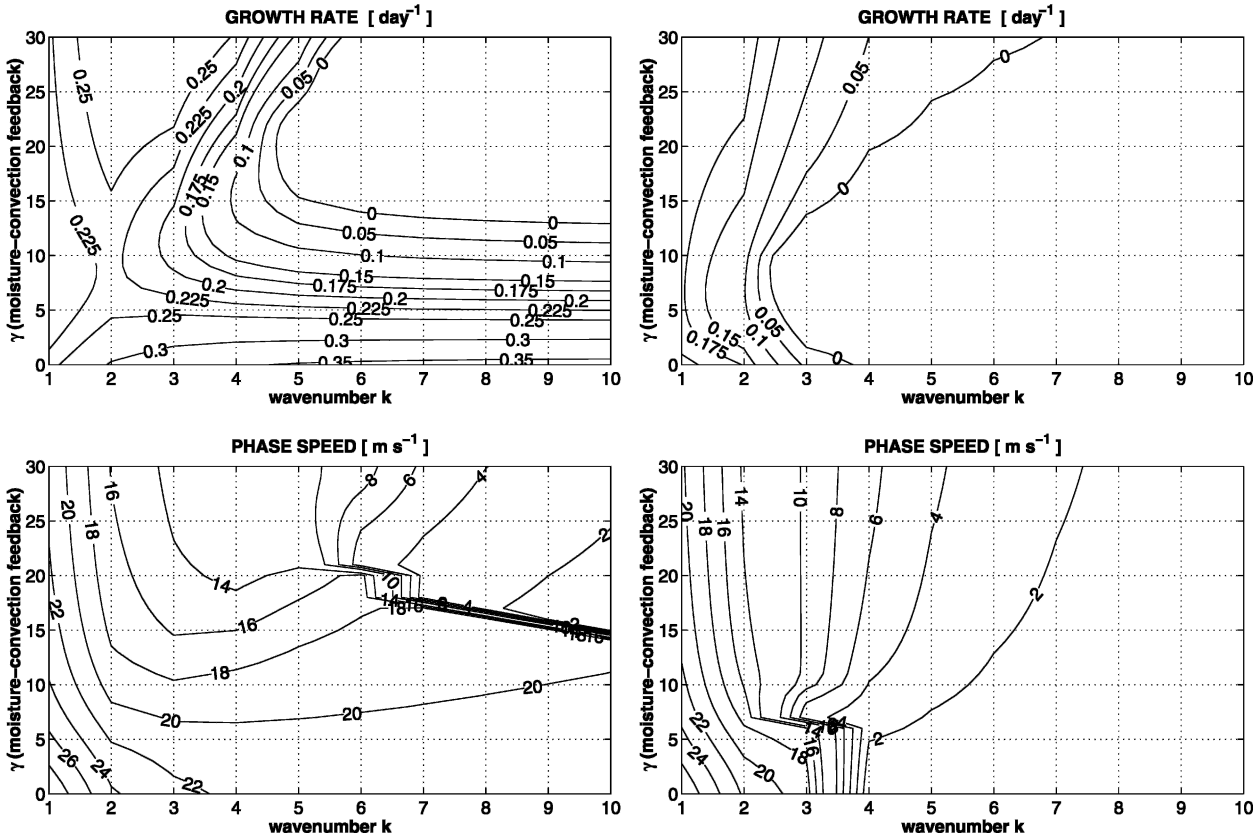

FIG. 8. (top) Growth rates (day^{-1}) and (bottom) phase speeds (m s^{-1}) of the dispersion equation solutions as a function of zonal wavenumber k and the intensity of the moisture-convection feedback γ in the absence of radiative feedback ($\alpha = 0$) for (left) $\tau_c = 0$ and (right) $\tau_c = 0.1$; $F = 0$, $\varepsilon_p = 0.8$, $\overline{U} = -5$ m s^{-1}.

ence of small-scale disturbances by radiative processes dominates.

On the other hand, although the two feedbacks individually slow down the propagation of planetary-scale disturbances, the moisture-convection feedback weakens the ability of radiative processes to slow down the propagation of planetary-scale disturbances. This is seen by comparing the influence of radiative feedbacks on phase speeds for different values of the moisture-convection feedback ($\gamma = 12$ in Fig. 9 and $\gamma = 0$ in Fig. 2). This may be understood by considering how convection affects the moist entropy deficit of the troposphere. On average, the moist entropy has a minimum in the middle troposphere and the vertically averaged moist entropy is smaller in the free troposphere than in the subcloud layer (Fig. 1). Therefore, upward convective motions increase the free tropospheric entropy while downward motions associated with shallow convective downdrafts and environmental subsidence decrease the subcloud-layer entropy. Vertical motions tend thus to oppose the moist entropy deficit of the troposphere. The modulation of the precipitation efficiency by moisture fluctuations amplifies the damping term of the perturbation entropy gradient between the subcloud layer and the free troposphere (section 2d), and hence amplifies that effect. The interaction between moisture and convection thus reduces the amplitude of the moist entropy deficit anomalies and with it the magnitude of the radiative feedback. This suggests that the variability of the tropical atmosphere depends on the relative strength of the moisture-convection and moisture–radiative feedbacks.

5. Summary and discussion

The objective of this study is to better understand the physical processes involved in the large-scale organization of the tropical atmosphere. We address in particular the role that atmospheric moisture (i.e., water vapor and clouds) may play at the intraseasonal time scale, through its interaction with radiation and convection. For this purpose, we use a simple linear model of the tropical atmosphere and consider a nonrotating two-dimensional atmosphere with constant background

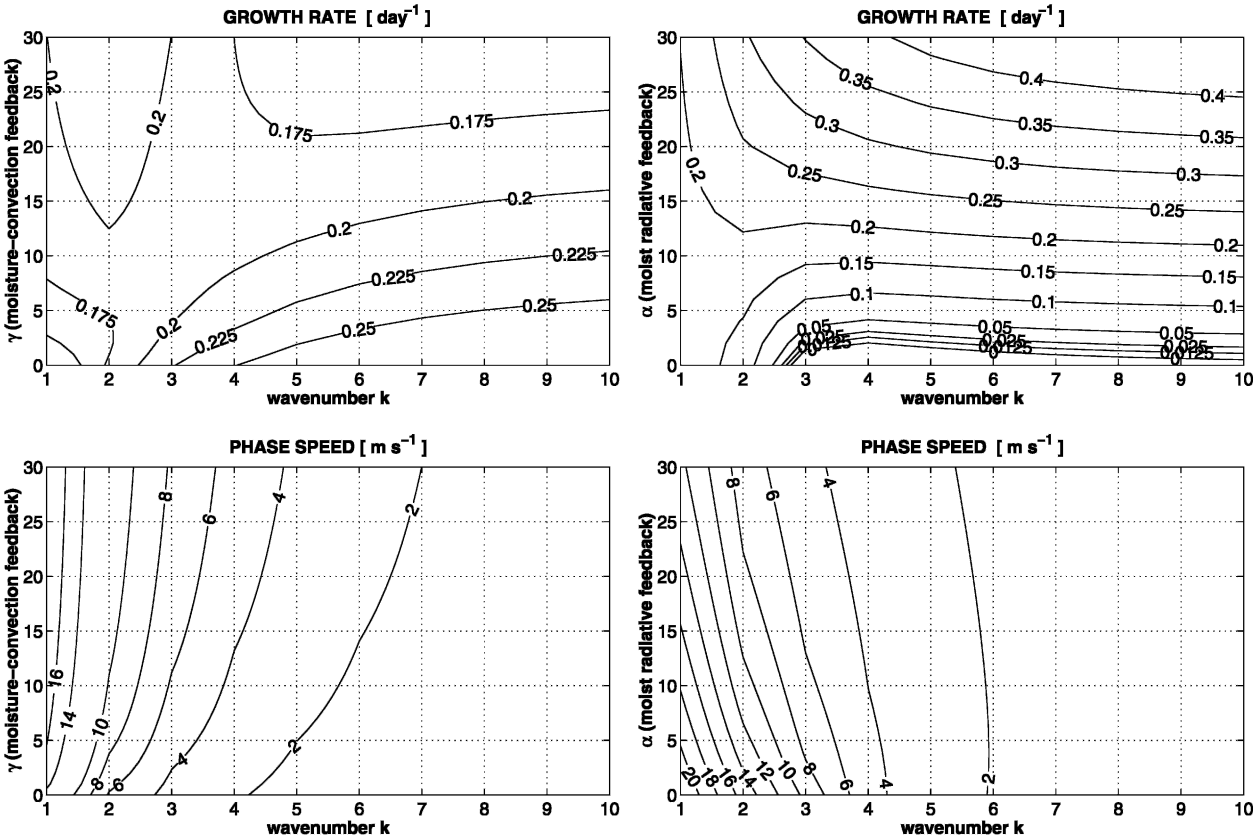

FIG. 9. (top) Growth rates (day^{-1}) and (bottom) phase speeds (m s^{-1}) of the dispersion equation solutions as a function of zonal wavenumber k and the intensity (left) of the moisture-convection feedback γ in the presence of moist–radiative feedbacks ($\alpha = 12$) and (right) of the moisture–radiation feedback α in the presence of moist-convection feedback ($\gamma = 12$). Qualitatively similar results are obtained for values of α and γ different from the value (12) chosen here; $\tau_c = 0.1$, $F = 0$, $\varepsilon_p = 0.8$, $\overline{U} = -5$ m s^{-1}.

wind and surface temperature. Cumulus convection is idealized as an ensemble of deep and shallow convective fluxes, with the assumption that the shallow updraft and downdraft are of equal mass flux. The total cumulus mass flux varies with the large-scale vertical motion of the atmosphere and surface heat fluxes, with a finite response time τ_c. Assuming that the temperature structure of the atmosphere is maintained at the moist adiabatic lapse rate, and that the convective neutrality of the troposphere is preserved, fluctuations of the atmospheric geopotential are linearly related to fluctuations of the subcloud-layer entropy. Moist-radiative feedbacks are introduced by assuming that the tropospheric radiative cooling varies linearly with the moist entropy deficit of the atmosphere (defined as the difference between the moist entropy of the subcloud layer and that of the free troposphere), so that an increase of the degree of saturation of the atmosphere leads to a weakening of the tropospheric radiative cooling, as observed in cloudy convective atmospheres. Finally, a feedback between moisture and convection is introduced by allowing the precipitation efficiency (defined as the ratio of the deep convective mass flux to the total updraft mass flux) to vary with the saturation deficit of the troposphere, so that it increases as the atmosphere gets closer to saturation. This effectively increases the sensitivity of convection to moisture perturbations.

Theoretical models of the tropical atmosphere have long represented radiative processes as a Newtonian cooling (e.g., Neelin and Yu 1994; Yano and Emanuel 1991). This yields radiative anomalies nearly in quadrature with vertical motion anomalies, and thus little effect on the propagation of the large-scale waves. But the present study, which assumes that radiation is modulated primarily by clouds, suggests that variable radiation owing to moisture–radiation feedbacks, has two important effects. The primary effect is to reduce the phase speed of large-scale tropical disturbances; by cooling the atmosphere less efficiently during the rising phase of the oscillations (when the atmosphere is moister) than during periods of large-scale subsidence

(when the atmosphere is drier), atmospheric radiative heating partly opposes the adiabatic temperature tendencies. This reduces the effective stratification felt by propagating waves and slows down their propagation. The second effect is to excite small-scale advective disturbances traveling with the mean flow. The variability of the equatorial atmosphere is thus likely to depend on the strength of moist–radiative feedbacks:

- In the presence of weak moist–radiative feedbacks, fast upwind propagating waves of planetary scale constitute the most unstable mode of the equatorial atmosphere. In that case, fluctuations of atmospheric moist entropy are found to be of smaller magnitude in the free troposphere than in the subcloud layer.
- In the presence of significant moist–radiative feedbacks, fluctuations of the free tropospheric moist entropy are of larger magnitude than that of the subcloud layer, and two unstable modes coexist: small-scale advective disturbances propagating along with the mean flow and slow planetary-scale disturbances propagating upwind at phase speeds ranging from a few m s^{-1} up to about 15 m s^{-1} (this corresponds to a period longer than about 30 days). However, in the presence of strong moist–radiative feedbacks, small-scale advective disturbances constitute the most unstable mode of the tropical atmosphere, and are likely to hide the planetary-scale organization of the equatorial atmosphere.

The moisture-convection feedback does not affect the existence of these two regimes. However, it favors the prominence of planetary-scale propagating waves at the expense of small-scale advective disturbances, and reduces the ability of radiative processes to slow down the planetary-scale disturbances by acting against the moist entropy deficit of the troposphere.

Our linear model of the tropical atmosphere assumes a nonrotating two-dimensional atmosphere having a uniform basic state with constant background easterlies.[3] Such an idealization precludes any claim that we are mimicking natural phenomena; our goal here is rather to understand the operation of a few fundamental physical processes within a deliberately simple framework. We believe we have helped identify several key processes that are critical for the tropical intraseasonal variability.

A robust observational finding is that the phase speed of tropical disturbances is smaller than that predicted by the equatorial Kelvin wave theory in a dry atmosphere (e.g., Wheeler and Kiladis 1999). Several studies propose that this is because the effective stratification of moist convective atmosphere is smaller than that of a dry atmosphere, owing to the heating of the troposphere by cumulus convection (Neelin and Yu 1994; Emanuel et al. 1994; Yu et al. 1998). The present study shows that the interaction of moisture (water vapor and clouds) with radiation may also contribute to this effect. This latter is expected to be particularly strong when the fluctuations of the moist entropy are of larger magnitude in the free troposphere than in the subcloud layer (Fig. 7). Such a feature is found when analyzing several years of data from an ensemble of tropical stations located in the Indian Ocean, Maritime Continent, and western Pacific Ocean (Figs. 3, 8, and 9 of Kemball-Cook and Weare 2001). Radiosonde data collected over the Pacific warm pool show that this was also the case during the TOGA COARE intense observing period (Fig. 1), when large-scale tropical oscillations were progressing eastward at about 6 m s^{-1} (Yanai et al. 2000).

Analyzing the observed OLR spectra of the equatorial atmosphere, Wheeler and Kiladis (1999) pointed out the presence of two main features classified as convectively coupled, but not corresponding to any equatorial wave predicted by the traditional linear wave theory: the MJO, with a zonal wavenumber-1–4 structure and propagating eastward with a period longer than 25 days, and westward moving synoptic-scale waves with periods around 3–6 days referred to as tropical depression-type disturbances (TD). Fully understanding these phenomena would require one to consider the complex three-dimensional structures of clouds and moisture (e.g., Wheeler et al. 2000; Sperber 2003). This is obviously not possible with our simple model. Nevertheless, the results of this study provoke us to speculate about the appearance of these phenomena in the equatorial spectrum.

This study suggests in particular that cloud-radiative processes can excite small-scale disturbances traveling with the mean flow. Perhaps this is related to the TD-type phenomena located away from the shallow water wave dispersion curves. Whether planetary intraseasonal waves correspond to moist Kelvin waves whose phase speed is affected by moist processes, or correspond to a fundamentally different phenomenon remains an open issue and a subject of investigation (Wheeler and Kiladis 1999; Lin et al. 2000; Frederiksen 2002). Nevertheless, Wheeler and Kiladis (1999) suggest that the MJO differs from the Kelvin wave signal

[3] Note that the effects of the moist-radiative and convective feedbacks on the organization of the tropical atmosphere described in this study do not depend on the direction of the mean background wind assumed in the model.

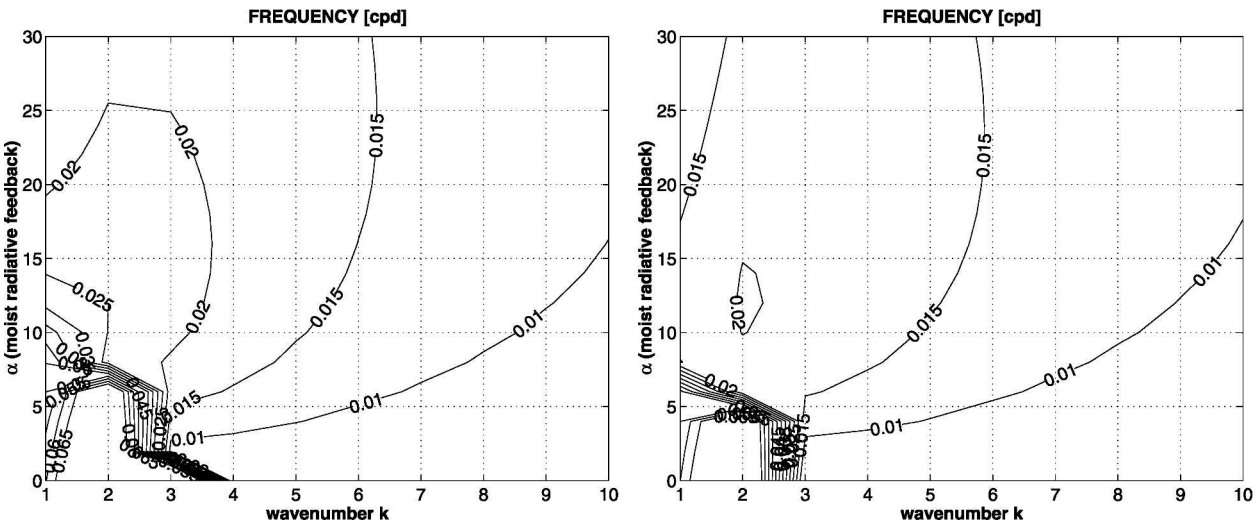

FIG. 10. Frequency (expressed in day^{-1}) predicted by the linear model as a function of the zonal wavenumber (k) and the strength of radiative feedbacks (α) (left) in the absence of surface friction ($F = 0$) and (right) in the presence of surface friction ($F = 0.2$); $\tau_c = 0.1$, $\varepsilon_p = 0.8$, $\overline{U} = -5$ m s^{-1}.

by having an approximately constant frequency around 0.025 cycles per day (cpd) for the range of zonal planetary wavenumbers 1 to about 7. Figure 10 shows that the planetary waves predicted by the linear model in the presence of significant moist radiative feedbacks are characterized also by an approximately constant frequency (around 0.015–0.020 cpd). These waves thus share an important attribute of MJO-like phenomena.

We now compare the results derived from our simple model with the findings of several recent studies using complex numerical models. Using an aquaplanet GCM, Lee et al. (2001) found that the feedback between clouds and longwave radiative forcing was responsible for the development of small-scale disturbances advected westward by the easterly flow, and for the slower propagation of eastward propagating disturbances of wavenumber 1. They showed in addition that the relative prominence, in the space–time spectrum of the tropical atmosphere, of small-scale advective disturbances and planetary-scale eastward propagating disturbances is highly sensitive to the intensity of cloud radiative feedbacks. These results are consistent with the effects of moist radiative feedbacks suggested by the present study. Simulations performed with a two-dimensional cloud-resolving model with prescribed radiation showed the development of systems of a few hundred kilometers scale traveling downwind, and of large-scale envelopes of convection of a few thousand kilometers propagating upwind (Grabowski and Moncrieff 2001). Grabowski and Moncrieff (2002) showed that the presence of interactive radiation adds perturbations of a few thousand kilometers in scale that are steered by the mean flow, and makes the large-scale envelopes of convection less coherent than in the case with prescribed radiation. These results are consistent with our finding that the presence of radiative feedbacks destabilizes small-scale disturbances traveling with the mean flow. However, in these simulations, as in those performed with the nonhydrostatic, cloud-resolving global model of Grabowski (2003), radiative feedbacks do not seem to have much effect on the phase speed of the large-scale envelopes of convection. On the other hand, the moisture-convection feedback seems essential for creating low frequency systems in this model (GM04). This suggests a strong moisture-convection feedback relative to the moisture-radiation feedback in these cloud-resolving model simulations, and the opposite in the GCM simulations of Lee et al. (2001).

The poor representation of tropical intraseasonal oscillations by large-scale numerical models (Slingo et al. 1996; Hendon et al. 2000; Jones et al. 2000), in particular the tendency of models to simulate oscillations that are too fast and too weak, led to the speculation that one or several physical components essential to the phenomenon could be misrepresented or missing in these models. The coupling between the ocean and the atmosphere has been proposed to be one of these components (e.g., Flatau et al. 1997; Sperber et al. 1997). However, if the representation of the interaction between the SST and the atmosphere actually improves the simulation of the MJO in some models (e.g., Waliser et al. 1999), there are other models

in which this does not appear to be the case (Hendon 2000). Many studies emphasize the sensitivity of the simulated intraseasonal variability to the representation of cumulus convection (e.g., Chao and Deng 1998; Wang and Schlesinger 1999; Maloney and Hartmann 2001). The recognition of the importance of moisture-radiation and moisture-convection feedbacks suggests that difficulties in simulating intraseasonal variability in the Tropics may be owing to poor representation of cloud–radiation interactions (Lee et al. 2001), a lack of sensitivity of parameterized convection to atmospheric moisture (Derbyshire et al. 2004; Grandpeix et al. 2004), or to coarse vertical resolution of climate models in the free troposphere.[4]

This study focused on the role of the atmospheric component of the cloud-radiation and moisture-convection feedbacks in a nonrotating atmosphere. However, the shading effect of clouds affects also the surface radiation budget, and convective downdrafts affect the surface evaporative cooling through their modulation of the subcloud-layer moist entropy. Therefore, a more complete investigation would require one to consider the combined effect of the atmospheric and surface components of the moist-radiative and moisture-convection feedbacks on tropical variability, at the equator and poleward. This will be pursued in a future study.

Acknowledgments. This work benefited from fruitful discussions with Jean-Louis Dufresne (LMD) and Arnaud Czaja (MIT). We thank Paul Ciesielski for providing the version 2 analysis of TOGA COARE data, and anonymous reviewers for their useful comments. We are grateful to Professors Peter Stone and John Marshall (MIT) for their support during this study through the MIT's Climate Modeling Initiative. The first author thanks CNRS (French National Center for Scientific Research) for permitting her to work at MIT during part of this work, and to the French PATOM and PNEDC programs for their support.

[4] Increasing the vertical resolution of the models in the free troposphere improves the representation of sharp temperature and humidity gradients, in particular near the freezing level (Tompkins and Emanuel 2000; Inness et al. 2001). This presumably constitutes a necessary condition for representing midlevel convection and associated cumulus congestus clouds, whose role in modulating the tropospheric radiative cooling and in moistening and preconditioning the atmosphere for deep convection at the intraseasonal time scale has been emphasized (Johnson et al. 1999; Inness et al. 2001).

REFERENCES

Bony, S., and K. A. Emanuel, 2001: A parameterization of the cloudiness associated with cumulus convection; evaluation using TOGA COARE data. *J. Atmos. Sci.,* **58,** 3158–3183.

Chao, W. C., and L. Deng, 1998: Tropical intraseasonal oscillation, super cloud clusters, and cumulus convection schemes. Part II: 3D aquaplanet simulations. *J. Atmos. Sci.,* **55,** 690–709.

Ciesielski, P. E., R. H. Johnson, P. T. Haertel, and J. Wang, 2003: Corrected TOGA COARE sounding humidity data: Impact on diagnosed properties of convection and climate over the warm pool. *J. Climate,* **16,** 2370–2384.

Derbyshire, S. H., I. Beau, P. Bechtold, J.-Y. Grandpeix, J.-M. Piriou, J.-L. Redelsperger, and P. M. M. Soares, 2004: Sensitivity of moist convection to environmental humidity. *Quart. J. Roy. Meteor. Soc.,* **30,** 3055–3079.

Emanuel, K. A., 1987: An air–sea interaction model of intraseasonal oscillations in the Tropics. *J. Atmos. Sci.,* **44,** 2324–2340.

——, 1993: The effect of convective response time on WISHE modes. *J. Atmos. Sci.,* **50,** 1763–1775.

——, J. D. Neelin, and C. S. Bretherton, 1994: On large-scale circulations in convecting atmospheres. *Quart. J. Roy. Meteor. Soc.,* **120,** 1111–1143.

Flatau, M., P. J. Flatau, P. Phoebus, and P. P. Niiler, 1997: The feedback between equatorial convection and local radiative and evaporative processes: The implications for intraseasonal oscillations. *J. Atmos. Sci.,* **54,** 2373–2386.

Frederiksen, J. S., 2002: Genesis of intraseasonal oscillations and equatorial waves. *J. Atmos. Sci.,* **59,** 2761–2781.

Fuchs, Z., and D. J. Raymond, 2002: Large-scale modes of a nonrotating atmosphere with water vapor and cloud radiation feedbacks. *J. Atmos. Sci.,* **59,** 1669–1679.

Grabowski, W. W., 2003: MJO-like coherent structures: Sensitivity simulations using the cloud-resolving convection parameterization (CRCP). *J. Atmos. Sci.,* **60,** 847–864.

——, and M. W. Moncrieff, 2001: Large-scale organization of tropical convection in two-dimensional explicit numerical simulations. *Quart. J. Roy. Meteor. Soc.,* **127,** 445–468.

——, and ——, 2002: Large-scale organization of tropical convection in two-dimensional explicit numerical simulations: Effects of interactive radiation. *Quart. J. Roy. Meteor. Soc.,* **128,** 2349–2375.

——, and ——, 2004: Moisture-convection feedback in the Tropics. *Quart. J. Roy. Meteor. Soc.,* **130,** 3081–3104.

Grandpeix, J.-Y., V. Phillips, and R. Tailleux, 2004: Improved mixing representation in Emanuel's convection scheme. *Quart. J. Roy. Meteor. Soc.,* **130,** 3207–3222.

Hendon, H. H., 2000: Impact of air–sea coupling on the Madden–Julian oscillation in a general circulation model. *J. Atmos. Sci.,* **57,** 3939–3952.

——, B. Liebmann, M. Newman, J. D. Glick, and J. Schemm, 2000: Medium-range forecast errors associated with active episodes of the Madden–Julian oscillation. *Mon. Wea. Rev.,* **128,** 69–86.

Inness, P. M., J. M. Slingo, S. J. Woolnough, R. B. Neale, and V. D. Pope, 2001: Organization of tropical convection in a GCM with varying vertical resolution; implications for the simulation of the Madden–Julian oscillation. *Climate Dyn.,* **17,** 777–793.

Johnson, R. H., and P. E. Ciesielski, 2000: Rainfall and radiative heating rates from TOGA COARE atmospheric budgets. *J. Atmos. Sci.,* **57,** 1497–1514.

——, T. M. Rickenbach, S. A. Rutledge, P. E. Ciesielski, and W. H. Schubert, 1999: Trimodal characteristics of tropical convection. *J. Climate,* **12,** 2397–2418.

Jones, C., D. E. Waliser, J.-K. E. Schemm, and W. K.-M. Lau, 2000: Prediction skill of the Madden and Julian oscillation in dynamical extended range forecasts. *Climate Dyn.,* **16,** 273–289.

Kemball-Cook, S. R., and B. C. Weare, 2001: The onset of convection in the Madden–Julian oscillation. *J. Climate,* **14,** 780–793.

Lee, M.-I., I.-S. Kang, J.-K. Kim, and B. E. Mapes, 2001: Influence of cloud-radiation interaction on simulating tropical intraseasonal oscillation with an atmospheric general circulation model. *J. Geophys. Res.,* **106,** 14 219–14 233.

Lin, J. W.-B., J. D. Neelin, and N. Zeng, 2000: Maintenance of tropical intraseasonal variability: Impact of evaporation–wind feedback and midlatitude storms. *J. Atmos. Sci.,* **57,** 2793–2823.

Madden, R. A., and P. R. Julian, 1971: Detection of a 40–50 day oscillation in the zonal wind in the tropical Pacific. *J. Atmos. Sci.,* **28,** 702–708.

——, and ——, 1972: Description of global-scale circulation cells in the Tropics with a 40–50 day period. *J. Atmos. Sci.,* **29,** 1109–1123.

——, and ——, 1994: Observations of the 40–50 day tropical oscillation—A review. *Mon. Wea. Rev.,* **122,** 814–837.

Maloney, E. D., and D. L. Hartmann, 2000: Modulation of hurricane activity in the Gulf of Mexico by the Madden–Julian oscillation. *Science,* **287,** 2002–2004.

——, and ——, 2001: The sensitivity of intraseasonal variability in the NCAR CCM3 to changes in convective parameterization. *J. Climate,* **14,** 2015–2034.

Mehta, A. V., and E. A. Smith, 1997: Variability of radiative cooling during the Asian summer monsoon and its influence on intraseasonal waves. *J. Atmos. Sci.,* **54,** 941–966.

Myers, D. S., and D. E. Waliser, 2003: Three-dimensional water vapor and cloud variations associated with the Madden–Julian oscillation during Northern Hemisphere winter. *J. Climate,* **16,** 929–950.

Neelin, J. D., and J. Y. Yu, 1994: Modes of tropical variability under convective adjustment and the Madden–Julian oscillation. Part I: Analytical results. *J. Atmos. Sci.,* **51,** 1876–1894.

——, I. M. Held, and K. H. Cook, 1987: Evaporation–wind feedback and low frequency variability in the tropical atmosphere. *J. Atmos. Sci.,* **44,** 2341–2348.

Parson, D. B., K. Yoneyama, and J.-L. Redelsperger, 2000: The evolution of the tropical western Pacific atmosphere–ocean system following the arrival of a dry intrusion. *Quart. J. Roy. Meteor. Soc.,* **126,** 517–548.

Raymond, D. J., 1995: Regulation of moist convection over the west Pacific warm pool. *J. Atmos. Sci.,* **52,** 3945–3959.

——, 2001: A new model of the Madden–Julian oscillation. *J. Atmos. Sci.,* **58,** 2807–2819.

Redelsperger, J.-L., D. B. Parson, and F. Guichard, 2002: Recovery processes and factors limiting cloud-top height following the arrival of a dry intrusion observed during TOGA COARE. *J. Atmos. Sci.,* **59,** 2438–2457.

Slingo, J. M., and R. A. Madden, 1991: Characteristics of the tropical intraseasonal oscillation in the NCAR community climate model. *Quart. J. Roy. Meteor. Soc.,* **117,** 1129–1169.

——, and Coauthors, 1996: Intraseasonal oscillations in 15 atmospheric general circulation models: Results from an AMIP diagnostic subproject. *Climate Dyn.,* **12,** 325–357.

Sperber, K. R., 2003: Propagation and the vertical structure of the Madden–Julian oscillation. *Mon. Wea. Rev.,* **131,** 3018–3037.

——, J. M. Slingo, P. M. Inness, and W. K.-M. Lau, 1997: On the maintenance and initiation of the intraseasonal oscillation in the NCEP/NCAR reanalysis and in the GLA and UKMO AMIP simulations. *Climate Dyn.,* **13,** 769–795.

Tompkins, A. M., 2001: Organization of tropical convection in low vertical wind shears: The role of water vapor. *J. Atmos. Sci.,* **58,** 529–545.

——, and K. A. Emanuel, 2000: The vertical resolution sensitivity of simulated equilibrium temperature and water-vapour profiles. *Quart. J. Roy. Meteor. Soc.,* **126,** 1219–1238.

Waliser, D. E., K.-M. Lau, and J.-H. Kim, 1999: The influence of coupled sea surface temperatures on the Madden–Julian oscillation: A model perturbation experiment. *J. Atmos. Sci.,* **56,** 333–358.

Wang, B., and X. Xie, 1998: Coupled modes of the warm pool climate system. Part I: The role of air–sea interaction in maintaining Madden–Julian oscillation. *J. Climate,* **11,** 2116–2135.

Wang, W., and M. E. Schlesinger, 1999: The dependence on convection parameterization of the tropical intraseasonal oscillation simulated by the UIUC 11-layer atmospheric GCM. *J. Climate,* **12,** 1424–1457.

Wheeler, M., and G. N. Kiladis, 1999: Convectively coupled equatorial waves: Analysis of clouds and temperature in the wavenumber-frequency domain. *J. Atmos. Sci.,* **56,** 374–399.

——, ——, and P. J. Webster, 2000: Large-scale dynamical fields associated with convectively coupled equatorial waves. *J. Atmos. Sci.,* **57,** 613–640.

Woolnough, S. J., J. M. Slingo, and B. J. Hoskins, 2000: The relationship between convection and sea surface temperature on intraseasonal time scales. *J. Climate,* **13,** 2086–2104.

——, ——, and ——, 2001: The organization of tropical convection by intraseasonal sea surface temperature anomalies. *Quart. J. Roy. Meteor. Soc.,* **127,** 887–907.

Yanai, M., B. Chen, and W.-W. Tung, 2000: The Madden–Julian oscillation observed during the TOGA COARE IOP: Global view. *J. Atmos. Sci.,* **57,** 2374–2396.

Yano, J.-I., and K. A. Emanuel, 1991: An improved model of the equatorial troposphere and its coupling with the stratosphere. *J. Atmos. Sci.,* **48,** 377–389.

Yu, J.-Y., and J. D. Neelin, 1994: Modes of tropical variability under convective adjustment and the Madden–Julian oscillation. Part II: Numerical results. *J. Atmos. Sci.,* **51,** 1895–1914.

——, C. Chou, and J. D. Neelin, 1998: Estimating the gross moist static stability of the tropical atmosphere. *J. Atmos. Sci.,* **55,** 1354–1372.